TOXICOLOGICAL SCIENCES **125(1)**, 91–104 (2012)
doi:10.1093/toxsci/kfr284
Advance Access publication October 20, 2011

TCDD Disrupts Hypural Skeletogenesis during Medaka Embryonic Development

Wu Dong,*,† David E. Hinton,‡ and Seth W. Kullman*,[1]

*Department of Environmental and Molecular Toxicology, North Carolina State University, Raleigh, North Carolina 27695; †Inner Mongolia Provincial Key Laboratory for Toxicants and Animal Disease, Inner Mongolia University for Nationalities, Tong Liao, China; and ‡Nicholas School of the Environment, Duke University, Durham, North Carolina 27708

[1]To whom correspondence should be addressed at Department of Environmental and Molecular Toxicology, North Carolina State University, Campus Box 7633, Raleigh, NC 27695. Fax: (919) 515-7169. E-mail: swkullma@ncsu.edu.

Received August 5, 2011; accepted October 12, 2011

Defective bone and cartilage development account for a large number of human birth defects annually. Normal skeletogenesis involves cartilage development in early morphogenesis through a highly coordinated and orchestrated series of events involving commitment and differentiation of mesenchymal cells to chondrocytes followed by a highly programmed process of structural maturation. Recent developmental studies with laboratory model fish demonstrate that exposure to 2,3,7,8-tetrachlorodibenzo-*p*-dioxin (TCDD) results in cartilage and skeletal abnormalities. In this study, we exposed embryonic medaka to TCDD to induce developmental modification(s) of both cartilage and bone formation. Emphasis is placed on cell-rich hyaline cartilage of the hypural plate where both chondrogenesis and osteogenesis are impaired by TCDD exposure. In this model, TCDD exposure results in a concentration-dependent impairment of mesenchymal cell recruitment, chondrocyte cell proliferation, differentiation, and progression to hypertrophy. Gene expression of ColA2, a marker of chondrocyte terminal differentiation in hypural structures, is markedly attenuated consistent with hypural dysmorphogenesis. Assessment of hypural structure using a transgenic medaka expressing mCherry under control of the *osterix* promoter illustrated significant attenuation in expression of the osteoblast gene marker and lack of formation of a calcified perichondral sheath surrounding hypural anlage. Overall, these studies illustrate that TCDD impacts terminal differentiation and growth of cartilage and bone in axial structures not likely derived from neural crest progenitors in medaka hypurals.

Key Words: **medaka; dioxin; cartilage; skeletogenesis; aquatic toxicology.**

2,3,7,8-Tetrachlorodibenzo-*p*-dioxin (TCDD or dioxin) is a widely studied polychlorinated aromatic compound known to impact reproductive, developmental, and cardiovascular systems in mammalian and model vertebrate species (Carney *et al*., 2006; Matsumura, 2009). TCDD mediates numerous biological effects via interaction with the aryl hydrocarbon receptor (AhR). AhR is a basic-helix-loop-helix Per-ARNT-Sim (bHLH-PAS) transcription factor and functions as a master regulator of drug metabolism and cell-regulatory signaling pathways including cell proliferation, differentiation, and apoptosis (Abel and Haarmann-Stemmann, 2010; Chopra and Schrenk, 2011). In addition to a role in adaptive and toxic responses to xenobiotics, physiological role(s) for AhR function in development have been recognized (Puga *et al*., 2009). Supporting evidence is derived from studies of AhR null mice (Fernandez-Salguero *et al*., 1996). While viable, such mice exhibit developmental and age-related alterations of cardiovascular, hepatic, reproductive, and immunological systems (Fernandez-Salguero *et al*., 1997). Additionally, AhR null mice are recalcitrant to dioxin toxicity and exhibit decreased developmental abnormalities following TCDD exposures (Peters *et al*., 1999).

Fish embryos are highly sensitive to TCDD at low ppt-ppb levels and exhibit significant developmental abnormalities including pericardial edema, reduced peripheral blood flow, craniofacial malformations, growth retardation, and death (Carney *et al*., 2006; Teraoka *et al*., 2003). These phenotypes are thought to arise from disruption in the balance of AhR signaling during development likely due to impairment of key regulatory processes associated with cell cycle, proliferation and differentiation, and cell death. Such impairment is thought to contribute to onset and progression of developmental dysmorphogenesis and disease (Abel and Haarmann-Stemmann, 2010; Puga, 2011).

Skeletal dysmorphogenesis, in particular disruption in craniofacial development, is among the earliest and most sensitive endpoints of TCDD toxicity in fish models (Henry *et al*., 1997; Hill *et al*., 2004; Hornung *et al*., 1999; Teraoka *et al*., 2006). Zebrafish AhR2 (one of three Ah receptors in zebrafish) mediates TCDD developmental toxicity in zebrafish and exhibits strong expression in developing lower jaw. However, the mechanism(s) of TCDD-induced jaw dysmorphogenesis remains unclear (Prasch *et al*., 2003; Teraoka *et al*.,

2002). Hornung *et al*., 1999 originally proposed that jaw malformation in lake trout was associated with TCDD-induced circulatory failure (Hornung *et al*., 1999). More recent studies in zebrafish demonstrated that circulation in the lower jaw was not affected until later stages of development (Teraoka *et al*., 2002). Subsequent investigations of jaw primordial cells demonstrated that disruption of cells within the neural crest significantly impacted craniofacial development. Ablation of the neural crest cells in defined regions of developing medaka (a teleost fish model) demonstrated that most of the anterior neurocranium and the entire viscerocranium received neural crest contributions during development including Meckels' and quadrate cartilage of the lower jaw, both targets of TCDD-induced cartilage dysmorphogenesis in zebrafish, medaka, and other teleost models (Langille and Hall, 1988; Teraoka *et al*., 2006; Yamauchi *et al*., 2006).

Cartilage development (chondrogenesis) is one of the earliest morphogenic steps in skeletogenesis (Hall, 2005; Zhang *et al*., 2009). Chondrogenesis consists of a highly coordinated and orchestrated series of events involving the commitment and differentiation of mesenchymal stem cells (MSCs) to chondrocytes, followed by a programmed and structured maturation including cell proliferation, differentiation, and hypertrophy (Hall and Witten, 2007). During embryonic development, mesenchymal cells differentiate giving rise to osteochondral precursors and cartilage anlage. In both teleosts and mammals, maturation of chondrocytes is accompanied by major changes in chondrocyte morphology, biosynthetic activity, and energy metabolism (Karsenty, 2008). In premineralized cartilage, component resting and proliferating chondrocytes are small and round. Then, these cells secrete a complex organic, extracellular matrix (ECM) that contains predominantly type II collagen and the proteoglycan aggrecan. As cartilage matures, chondrocytes undergo hypertrophy resulting in an increased cell diameter and volume. These changes are accompanied by alterations in protein expression and energy metabolism as hypertrophic chondrocytes have a high-energy demand for maintenance of their cell volume and synthesis of the ECM.

To better understand targets and mechanisms of TCDD-induced developmental toxicity, we tested the hypothesis that early embryonic exposures to TCDD impact skeletogenesis in the axial skeleton of the medaka caudal peduncle comprised cell-rich hyaline cartilage (CRHC). Abundant CRHC is found in teleost jaw and hypural structures of the medaka caudal peduncle. We have chosen to investigate CRHC within medaka hypurals due to the fact that these structures are not derived from neural crest progenitors (compared with jaw), but they contain abundant numbers of chondrocytes that progress through a defined chondrogenic program including commitment and differentiation of mesenchymal cells to chondrocytes, maturation and hypertrophy and formation of a calcified perichondrium. Using high-resolution imaging of the hypural structures, we define a novel phenotype of TCDD cartilage dysmorphogenesis. This phenotype is anchored through gene expression analysis of chondrocyte (COL2A1) and osteoblast (Osterix) specific cell markers. COL2A1 was chosen, as a marker of chondrogenesis based upon its defined expression in terminally differentiated chondrocytes and regulation by SOX9, a known target of TCDD in jaw dysmorphogenesis in zebrafish (Xiong *et al*., 2008). Osterix gene expression was investigated due to its critical role in osteoblast differentiation using a transgenic medaka model that expressed mCherry under regulatory control of the *Osx* promoter. Use of this model enables sensitive detection of *Osx* gene expression in all medaka skeletal elements during embryogenesis (Renn and Winkler, 2009). Overall, these studies illustrate that TCDD impacts growth and differentiation of cartilage and bone cell types in axial structures not likely derived from neural crest progenitors.

MATERIALS AND METHODS

Medaka culture and embryo collection. Fish care and maintenance was provided daily in accordance with North Carolina State University IACUC approved animal protocols (NCSU# 07-183-B). Broodstock were housed in an enclosed recirculating aquatic system with charcoal filtration and UV treatment used in each passage. Water temperature and pH, monitored daily, were maintained at ~25 ± 2°C and ~7.4, respectively, and broodstock were maintained under a strict light:dark cycle of 16:8 h. Dry food (Otohime B1; Reed Mariculture, Campbell, CA) was fed several times per day via automated feeders with once daily supplementation of newly hatched *Artemia nauplii*. Under the care and culture conditions described above, medaka spawned daily and masses of embryonated eggs (20–30 per mass) were collected and separated (disruption of attachment filaments joining individual eggs) by gentle rolling on a moistened surface. Groups of individual embryonated eggs of specified collection date and developmental stage (Iwamatsu, 2004) were suspended in a 2% saline solution made from Instant Ocean (Aquatic Ecosystems, Apopka, FL) in a 100 × 20-mm tissue culture dish (BD Biosciences, Franklin Lanes, NJ) and housed at 26°C under gentle movement. After 5 days, marine water was replaced with 1× embryo rearing medium (ERM) containing 17.1mM NaCl and, in micromolars, 272 $CaCl_2{\cdot}2H_2O$, 402 KCl, and 661 $MgSO_4{\cdot}7H_2O$ through hatching (usually 9 days postfertilization [dpf]). Grow out of medaka embryos up to 10 dpf was performed in 6-well tissue culture plates containing 100 ml 1× ERM. Embryos were examined under a dissecting microscope, for morphological changes and described phenotypes. *Osx*-mCherry medaka were obtained from Dr Christoph Winkler, Department of Biological Sciences, National University of Singapore and cultured as described above for orange red medaka.

Chemicals. TCDD (or dioxin) (99% purity) was purchased from Cambridge Isotope Laboratories (Andover, MA). Alizarin Red and Alcian Blue were purchased from Sigma-Aldrich, St Louis, MO.

Exposures. Medaka embryos 4- to 5-h postfertilization (hpf) (stages 8–9) were collected and processed as described above. All exposures were conducted in Corning 6-well tissue culture plates (Corning, NY). For each exposure, embryos were treated in three replicate experimental wells containing 10 embryos per well, and each experiment was replicated 3 or more times. Embryos were exposed to a concentration of TCDD between 0.01 and 1 ppb for a duration of 1 h followed by replicate rinses (3×) with 1× ERM. Individuals were maintained in ERM with daily replacement for a total of 10 days, at which time they were processed for morphological or gene expression analysis.

Total RNA isolation. RNA was extracted from caudal peduncles of 10-dpf medaka exposed as described above to either dimethyl sulfoxide (DMSO)

vehicle (control) or TCDD. Each caudal peduncle was transected using a clean new razor blade previously treated with RNaseZAP (Sigma) and diethylpyrocarbonate-treated sterile deionized water. Care was taken to collect a peduncle of 1 mm length containing five to seven vertebral bodies and the caudal-most margin containing hypural cartilage structures. Next, peduncles were homogenized with 1 ml of RNA Bee (TelTest, Friendswood, TX) using a stainless steel Polytron homogenizer (Kinematica, Newark, NJ) treated as above. Following homogenization, total RNA was isolated as described previously (Dong *et al*., 2010). Prior to sample elution, each sample was on column–digested with DNase to eliminate DNA contamination using an RNase-free DNase Set according to manufacturer's instructions (Qiagen, Germantown, MD) and then eluted with 30 µl of warmed (52°C) RNase-free water. RNA quantity and 260/280 ratios were determined using a NanoDrop ND-1000 spectrophotometer (ThermoFisher Scientific, Inc., Pittsburgh, PA).

Quantitative real-time PCR. Synthesis of complementary DNA (cDNA) was conducted with 250 ng total RNA using High Capacity cDNA Reverse Transcription Kit (Applied Biosystems, Foster City, CA) containing random primers, MultiScribe Reverse Transcriptase, RNase inhibitor, deoxynucleotide triphosphate mix, and 10X reverse transcription buffer in a 20 µl reaction. Relative levels of *Col2a1* (1 of 2 and 2 of 2), *Cyp1A1*, and *18s* transcripts in DMSO- and TCDD-treated caudal peduncles were measured using quantitative real-time PCR (qPCR). The following medaka-specific real-time PCR primers were designed using PrimerQuest (Integrated DNA Technologies, Coralville, IA): *Cyp1A1*, forward primer 5′-ACATCGGCCTGAACCGAAATCCTA-3′, reverse primer 5′-TGCTTCATTGTGAGCCCGTACTCT-3′; *Col2a1* 1 of 2, forward primer 5′-GCTGCGGATGTTCTCAATCT-3′, reverse primer 5′-ATTGACATGTCTGCGTTTGC-3′; *Col2a1* 2 of 2, forward primer 5′-ACAGCCGCTTCACCTACAGT-3′, reverse primer 5′-GGGCCTATGTCAACTCCAAA-3′; *Sox9a*, forward primer 5′-CAGCTACAGCGGCAACTACA-3′, reverse primer 5′-GCTGCTCCGTCTTAATCTGG-3′; *Sox9b*, forward primer 5′-AAAGCCAACAGGGTCAACAG-3′, reverse primer 5′-GCTGTAGTAAGAGTTGGCAC-3′; and *18s*, forward primer 5′-CCTGCGGCTTAATTTGACTC-3′, reverse primer 5′-GACAAATCGCTCCACCAACT-3′. *Cyp1A1*, *Col2a1* (1 of 2 and 2 of 2), *Sox9a/b* and *18s* cDNAs were PCR amplified separately in triplicate using a 96-well PCR plate and an ABI PRISM 7000 Sequence Detection System (Applied Biosystems). For each 25-µl real-time PCR reaction, cDNAs were amplified using 1 µl (1 ng/µl) first-strand cDNA, 9.5 µl RNase-free water, 1 µl 5 µM forward primer, 1 µl 5 µM reverse primer, and 12.5 µl 2× QuantiTect SYBR Green PCR Master Mix (Qiagen, Inc., Valencia, CA). Real-time PCR reaction conditions were 95°C for 15 min followed by 41 cycles of 94°C for 15 s, 55°C for 30 s, and 72°C for 1 min. Relative quantitation of gene expression within each reaction was calculated following manufacturer's instructions (User Bulletin #2, ABI PRISM 7700 Sequence Detection System, Applied Biosystems, Foster City, CA). For each sample, the threshold cycle for reference (*18s*) amplification (C_t, *18s*) was subtracted from the threshold cycle for target amplification (C_t, *Cyp1A1*, *Sox9a/b* or *Col2a1*) to yield a ΔC_t. The threshold cycle represents the cycle number at which the fluorescence signal is significantly above the baseline. The mean or SD of ΔC_t for DMSO-treated samples was subtracted from the mean or SD of ΔC_t for TCDD-treated samples to yield a mean and SD of $\Delta\Delta C_t$ for each target. Fold induction relative to DMSO-treated individuals and 95% CIs were calculated using $2 - \Delta\Delta^{C_t}$ (Livak and Schmittgen, 2001).

In situ *hybridization.* Whole-mount *in situ* hybridization (ISH) was carried out as previously described (Dong *et al*., 2002). Probe constructs were generated by PCR amplification of medaka *Col2a1* (1 of 2 and 2 of 2) from a medaka cDNA library. The *Col2a1* 1 of 2 probe construct consists of 476 bp (forward primer 5′-AACATGGAGACAGGGGAGTCC-3′, reverse primer 5′-TGG TCC GCT CCA CCA ATA TC-3′) and the *Col2a1* 2 of 2 probe construct consists of 354 bp (forward primer 5′-GAATCAGCAAAGTACCAAAG-3′, reverse primer 5′-ACC GGC CTG AAT GCC TCT T-3′). Probe constructs were purified and subcloned in pGEM-TEasy Vector (Promega, Madison, WI). Antisense and sense digoxigenin labeled probes were synthesized by *in vitro* transcription using T7 and SP6 polymerase on template DNA linearized with AatII or ApaI, respectively. Medaka embryos (4 dpf) were fixed in 4% paraformaldehyde (PFA) for 24 h at 4°C, rinsed twice in PBS, and treated with proteinase-K (Sigma) in PBS with 0.1% Tween (PTw) for 1 h. After incubation with hybridization buffer containing (50% formamide, 5× SSC, 2 mg/ml Torula RNA (Sigma), and 200 mg/ml heparin), embryos were hybridized with antisense probes of medaka *Col2a1* (1 of 2 and 2 of 2) at 65°C overnight. Following hybridization, embryos were washed with 2 × SSC and 0.2 × SSC for 30 min, twice, at 65°C, respectively. After blocking with buffer containing 2% blocking reagent (Roche, Nutley, NJ) in 100mM maleic acid (pH 7.5) and 150mM NaCl, embryos were incubated with 1:4000 diluted anti-DIG antibody conjugated with alkaline phosphatase (Roche) at 4°C overnight. The color reaction was carried out by incubation in BM-purple substrate (Roche) after equilibration with NTMT buffer (100mM NaCl, 100mM Tris-HCl, pH 9.5, and 50mM $MgCl_2$) at room temperature. After PFA fixation, the stained embryos were cleared in 70% glycerol and directly observed and photographed.

Cartilage and bone staining. Medaka embryos 10 dpf were stained with Alcian Blue and/or Alizarin Red according to the method of Inohaya and Kudo (2000). Briefly, embryos were fixed in 4% PFA for 24 h at 4°C, rinsed twice in PBS, and stained by emersion in 0.1% Alcian Blue 8GX/80% ethanol/20% acetic acid for 6 h. After a series of washes with 75 and 50% ethanol/PBS each for 1 h, embryos were incubated with PBS overnight. For clarification, embryos were treated with 1% KOH/3% H_2O_2 for 20 h, followed by digestion with 0.05% trypsin/saturated tetraborate for 1 h, and staining in Alizarin Red solution (2 ml saturated Alizarin Red S in ethanol/8 ml 0.5% KOH) at room temperature until bones were distinctly red. Embryos were then washed 2× in 0.5% aqueous KOH, placed in 80% glycerol solution, directly observed and photographed.

Immunohistochemistry staining. Whole-mount immunohistochemistry (WIHC) was performed on medaka embryos 10 dpf for detection of COL2A1 as previously described (Dong *et al*., 2004). Briefly, 4% PFA fixed embryos were treated with proteinase-K in PBS for 1 h and rinsed with PBS containing 0.5% Triton X-100 and 1% DMSO (PBTD). After blocking with 3% normal BSA in PBTD, embryos were incubated overnight with mouse anti-COL2a1 antibody (anti-type II collagen, monoclonal antibody at 1:100, from the Developmental Studies Hybridoma Bank, Department of Biological Sciences, University of Iowa, Iowa City, IA). After washing in PBTD for several hours, embryos were treated with biotin-conjugated anti-mouse IgG antibody (1:200; Sigma), followed by overnight incubation with AB solution contained within the Vectastatin Elite kit (Vector Laboratories, Ltd.). Color reaction was performed with diaminobenzidine tetrachloride (DAB) and H_2O_2. For control, secondary antibody was omitted. After PFA fixation, the stained embryos were cleared in 70% glycerol and directly observed and photographed as a whole mount.

Immunohistochemistry was conducted with 4% PFA fixed paraffin-embedded 5-µm sections of vehicle and TCDD-exposed medaka embryos. These were mounted on glass histological slides, incubated with PBS with 0.5% Triton X-100 and 1% horse serum (PBTR) for 30 min after proteinase-K treatment. Next, sections were incubated with either anti-PCNA (mouse monoclonal anti-PCNA antibody, 1:500; Dako, Carpinteria, CA) or anti-RFP antibody (mouse monoclonal anti-RFP antibody; Abcam, Cambridge, MA) overnight at 4°C, followed by goat anti-mouse HRP-conjugated IgG (1:200; Dako) or HRP-conjugated anti-mouse IgG antibody (1:200), respectively. In control preparations, secondary antibody was omitted. After washing with PBTR, sections were reacted with a Vectastatin Elite kit (Burlingame, CA) according to manufacturer's instructions. Color reaction was performed with DAB and H_2O_2. Sections were mounted, coverslipped, and imaged using standard methods (Dong *et al*., 2002).

Glycol methacrylate embedment. To increase resolution of hypural morphologic assessments, the water-soluble monomer glycol methacrylate (GMA) in Technovit 7100 GMA Kit from EBSciences, East Granby, CT was used. Individual control and TCDD-treated ($n = 15$ per exposure) embryos (10 dpf) were transferred to ice cold 1× ERM for anesthesia and then immersed in 10 volumes of 4% PFA fixative and held at 4°C until processing (Passeri *et al*., 2009). Dehydration, infiltration, and hardening followed the

manufacturer's recommendations. A Leica 2065 Supercut Microtome (Leica Microsystems Inc., Bannockburn, IL) with a knife holder for triangular glass knives was used for sectioning (2.5 μm thickness). Sections were mounted, coverslipped, and imaged using standard methods (Dong *et al*., 2002).

Transmission electron microscopy. Transmission electron microscopy (TEM) was used to provide optimal resolving power of developing hypural structures. Dechorionated embryos 10 dpf were anesthetized and immediately fixed by immersion in 4% PFA/1% glutaraldehyde, in 0.1M cacodylate buffer pH 7.2–7.4 (4F:1G) at 4°C until processing. After rinsing (2×) in 0.1M sodium phosphate buffer (pH 7.2–7.4), samples were postfixed in 1% osmium tetroxide/0.1M sodium phosphate buffer (pH 7.2–7.4) for 1 h at room temperature. Resultant secondarily fixed embryos were then rinsed 2× in distilled water, dehydrated in graded ethanol solutions, rinsed 2× in 100% acetone, placed in a 1:1 mixture of Spurr's resin and acetone for 30 min, and then transferred to 100% Spurr's resin for 1 h. After an initial incubation, embryos were incubated in a new solution of 100% Spurr's resin for 1 h, placed in molds, and polymerized at 70°C overnight. Semithin sections (500 nm thick) were cut with glass knives and stained with 1% toluidine blue O in 1% sodium borate. These sections served two purposes. First, to determine presence of caudal peduncle and components in section plane and second, to provide the highest resolution light microscopy. Once hypural structures were shown to be present in semithin sections, ultrathin sections (70–90 nm thick) were cut with a diamond knife, placed on copper grids, stained with methanolic uranyl acetate and lead citrate, and imaged as below.

Imaging. Hypural structures were imaged with either a Nikon SMZ1500 camera equipped with a Nikon digital camera (digital sight DS-Fi1, Kanagawa, Japan) and Nikon NIS-Elements imaging software (Nikon, Melville, NY) or with a Nikon Eclipse E600 light microscope, a Nikon DXM 1200 digital camera, and EclipseNet imaging software (Nikon). TEM was conducted using a FEI/Philips EM 208S transmission electron microscope at 80 kV accelerating voltage. All TEM processing, analysis, and imaging were performed at the Laboratory for Advanced Electron and Light Optical Methods (LAELOM), College of Veterinary Medicine, North Carolina State University. All morphometric areal analyses of hypural images were performed using Image J (National Institutes of Health, Bethesda, MD) and area (square microns) of hypural was estimated using a cursor under 100× total magnification. Total area was determined based on the original image scale and planar analysis and estimates were based on the mean ± SEM of 10 embryos for each concentration.

Statistical analysis. Real-time PCR data and TCDD-induced tail phenotypes were tested for significant differences within treatment using a Prism4 software package (GraphPad Software Inc., San Diego, CA). Data were logarithmically transformed as needed to improve equality of variances (ANOVA, p value < 0.05), followed by Newman-Keuls Multiple Comparison test. Each qPCR experiment was performed with 3 biological replicates of 10 pooled embryos, and each qPCR amplification was conducted in triplicate.

RESULTS

Medaka Hypural Phenotypes

Medaka hypural morphology was assessed by double staining caudal peduncles in fish at 10 dpf with both Alcian Blue (for cartilage) and Alizarin Red (mineralized bony structures) stains. As demonstrated in Figure 1A, the caudal complex of medaka consists of two hypural structures that have formed ventral to the caudal notochord and support extension of related fin rays. From a lateral view at 10 dpf (Fig. 1A), the lower hypural plate (HP1) is the largest resulting from fusion of the first and second hypurals. The upper (i.e., dorsal) smaller hypural plate (HP2) is a fusion of the third, fourth, and fifth hypurals. Ventral to HP1 is the parahypural (PH). PH appears to be separating from the notochord with one caudal ray extending from it. Also visible is the cartilaginous bud of the hemal arch of the second preural centrum (HAPU2) and a small cartilaginous epural plate (EP1) dorsal to the notochord. At 10 dpf, neural and hemal arches are not well formed, however, notochord flexation is well pronounced. Moderate to no Alizarin Red staining is observed in preural centrum, ventral margins of centra, and neural and hemal arches, suggesting that mineralization has not yet occurred in these structures. At 10 dpf, there was additionally no evidence of formation of the first ural centrum as described by Fujita (1992).

Embryos exposed to TCDD between 0.05 and 1 ppb for 1 h at 4 hpf and then grown in clean ERM for 10 days revealed significantly disrupted hypural formation. As illustrated in Figures 2B–H, Alcian Blue-stained peduncles from embryos at 10 (dpf) demonstrated marked reduction in hypural structures

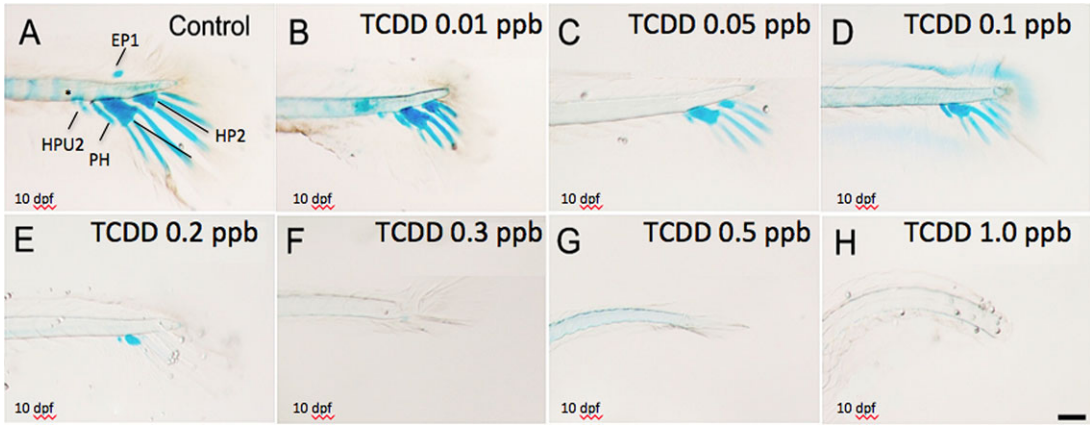

FIG. 1. Inhibitory effect of TCDD on medaka hypural development. Medaka embryos were exposed to vehicle or graded concentrations of TCDD (0.01–1 ppb) at 4 hpf for 1 h. Next, they were washed and incubated in ERM at 26°C until 10 dpf. Caudal peduncle containing axial skeleton was double stained with Alcian Blue and Alizarin Red at 10 dpf for visualization of hypural structures. Representative figures are shown. (A) Lateral view of hypurals structure in control animals. Caudal peduncle containing axial skeleton including: EP1, epural plate; HP1, Hypural 1; HP2, Hypural 2; HAPU2, the second preural centrum; PH, parahypural. (B–H) Lateral view of hypurals in TCDD-exposed animals at 10 dpf. Bar = 100 μm.

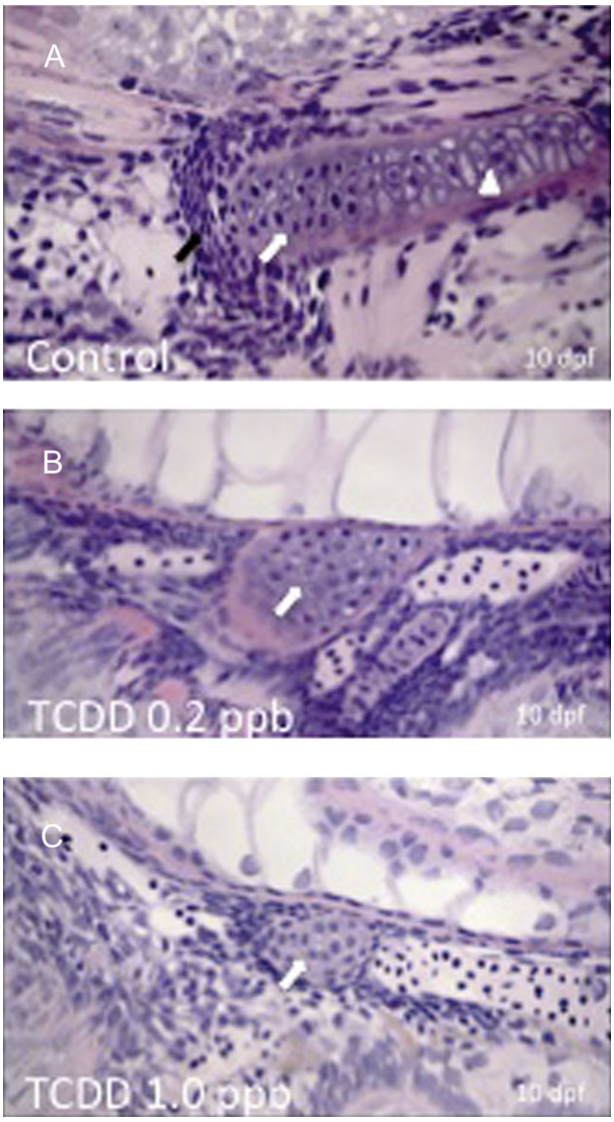

FIG. 2. Histological assessment of hypural phenotypes in GMA sections of control and treated embryos stained with H&E. A total of five embryos were analyzed at each concentration and the images shown are representative of all animals within a given group. Orientation of images is such that head is to the right, dorsal is at top, and ventral is toward bottom of figure with caudal peduncle to the left. Medaka embryos were exposed to DMSO (A), 0.2 ppb TCDD (B), or 1 ppb TCDD (C) at 4 hpf for 1 h, washed, and incubated in ERM at 26°C. At 10 dpf, embryos were dechorionated, fixed, and embedded in GMA followed by sectioning at 2.5 μm. Black arrows indicate presence of mesenchymal cell condensations. White arrows indicate differentiated chondrocytes within hypural structures. White arrowhead indicates hypertrophic chondrocytes within hypurals of control group. Note near absence of mesenchymal cells in B and C. Bar = 100 μm.

between controls and treated groups. Hypural defects were apparent at a concentration of 0.05 ppb TCDD and progressed in a concentration-related manner up to 0.3 ppb TCDD where little to no cartilage (Alcian Blue) staining was visible. At a concentration of 0.01 ppb TCDD, a complete loss of epural (EP1) development was observed with marked reduction in extension and staining of caudal fin rays. A TCDD concentration of 0.1 ppb resulted in an absence of HP2 development with significantly reduced staining in HP1. Minimal Alcian Blue staining was observed in all, but the parahypural at 0.2 ppb TCDD and a complete deficit in hypural structural development characterized all embryos exposed to TCDD concentrations greater than 0.3 ppb.

Histological Assessment of Hypural Phenotype-GMA Sections and Hematoxylin and Eosin Staining

Histological assessment of medaka embryonic (10 dpf) hypural phenotypes was conducted in GMA sections (Fig. 2). The added resolution, afforded by this approach, aided assessment of chondrocyte cell structure and morphology in the hypural regions. Using standard hematoxylin and eosin (H&E) staining, well-defined hypural structures including hypurals HP1, HP2, and parahypural (PH) were observed in addition to a well-formed notochord. In control animals, chondrocytes were apparent in each of the hypural and parahypural structures and observed as large disk shaped cells oriented in a stacked linear fashion. Cells revealed features of differentiation and hypertrophy consistent with relevant cellular modifications of chondrogenic differentiation (Hickok *et al.*, 1998). TCDD-treated animals exhibited a marked reduction in development of hypural structures. At a concentration on 0.2 ppb TCDD, minimal hypural structure was discerned. One cartilaginous structure was observed, consistent with observations made with Alcian Blue staining in Figure 1. This structure was both ventral and rostral to the tip of the peduncle and was adjacent to the notochord indicating that it is either parahypural or HP1 in origin. Cells in this structure were small condensed mesenchymal cells with little accumulation of ECM proteins. Cells were greatly reduced in number under this condition and had not differentiated or undergone morphogenesis to form stacks of chondrocytes, seen in control individuals. Exposure to > 0.2 ppb TCDD resulted in further deficits in development of hypural structures, this time with no apparent accumulation of caudal hypertrophic chondrocytes.

TEM of Hypural Cartilage

To further assess structural modifications in hypural structures, we conducted transmission electron microscopic analysis of control and treaded medaka embryos 10 dpf. Ultrastructure of medaka hypural showed cartilage structures and cellular zonation. In control animals (Figs. 3A and 3B), we observed a substantial zone of mesenchymal cell condensation consisting of elongated cuboidal-like cells at the periphery of the cartilaginous structure. Within the cartilage anlage, a transition toward ovoid to elongated irregularly shaped cells with small nuclei was observed. These cells were seen to further differentiate into well-defined cells with large dense nuclei typical of differentiated chondrocytes. Hypertrophic chondrocytes were visible well within cartilage anlage

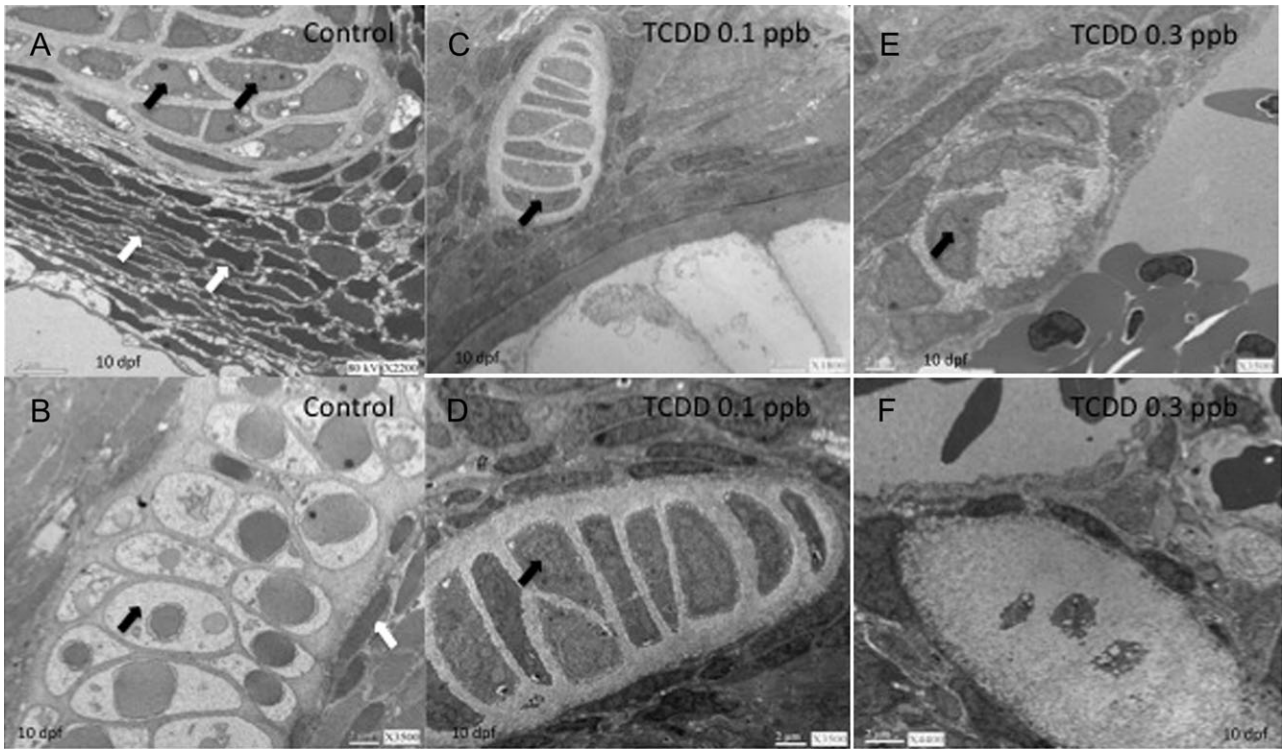

FIG. 3. Ultrastructure of medaka hypural. Embryos were exposed to either DMSO (vehicle control), 0.1 ppb TCDD, or 0.3 ppb TCDD at 4 hpf for 1 h, washed, and incubated in ERM at 26°C until 10 dpf. Then, embryos were manually dechorionated, fixed, and processed for TEM. (A and B) DMSO control; (C and D) 0.1 ppb TCDD; (E and F) 0.3 ppb TCDD. White arrows in panel A indicate mesenchymal cell condensations. Black arrows indicate differentiated chondrocytes in panels A–E. Note that cartilage structure in panels C–E are smaller than those of control (panels A and B) and contain fewer well-differentiated chondrocytes. Black arrow in panel B indicates hypertrophic chondrocytes. Chondrocytes of F appear to be arrested in growth and differentiation. Magnifications for panels are (A) 2200×, (B) 3500×, (C) 1800×, (D) 3500×, (E) 3500×, and (F) 4400×.

(Fig. 3B). Nuclei of the hypertrophic cells possessed a defined outer nuclear envelope and cytosol appeared vacuolated and filled with collagen fibrils. A dense ECM was apparent between differentiated chondrocytes. At 0.1 ppb TCDD, medaka hypurals appeared as small partially defined structures containing few organized stacks of differentiated chondrocytes (Figs. 3C and 3D). There was limited production of ECM within the cartilage anlage, and structures lacked obvious features of mesenchymal cell condensation and progression toward well-differentiated and hypertrophic chondrocytes. At a higher concentration (0.3 ppb TCDD), hypural structures were ill defined, containing only a few irregular poorly differentiated chondrocytes (Figs. 3E and 3F). Sparse ECM was seen; however, fibrils appeared thicker and fragmented when compared with control structures.

WIHC and ISH of Col2A1

To assess the impact of TCDD on deposition of ECM proteins, we next examined expression of protein type II collagen (COL2A1). Type II collagen, a major ECM protein, was assessed as a molecular marker of cartilage development and deposition in hypural structures. Type II collagen expression was determined at both the protein and the messenger RNA (mRNA) level using WIHC and ISH. In the former, a polyclonal antibody from the Developmental Studies Hybridoma Bank was used. As demonstrated in Figures 4A and 4B, type II collagen was abundantly expressed throughout the entirety of each hypural structure of control 10 dpf larvae. Staining was most intense at the periphery of hypural structures and was present within each defined chondral plate including parahypurals, HP1, HP2, and the epural. Some collagen staining was observed in the notochordal sheath as described by Ohisa *et al*. (2010). Following TCDD exposure (1 ppb), 10-day medaka lacked formation of defined hypural structures and exhibited a complete deficit in COL2A staining.

Given that medaka possess duplicate forms (paralogs) of *Col2A1*, ISH was conducted to determine if differential expression of the gene duplicates was impacted by TCDD treatment during early development. In control 4 dpf embryos, expression of *Col2A1* duplicates (*Col2A1* 1 of 2 and *Col2A1* 2 of 2) was observed in chondrogenic and nonchondrogenic tissues including the notochord, otic vesicle, and developing fins. The pattern was similar to that observed in similarly reacted zebrafish (Lele and Krone, 1997; Tilton *et al*., 2006). Little difference was observed in global expression patterns of the duplicates suggesting that, in normalcy, subfunctional

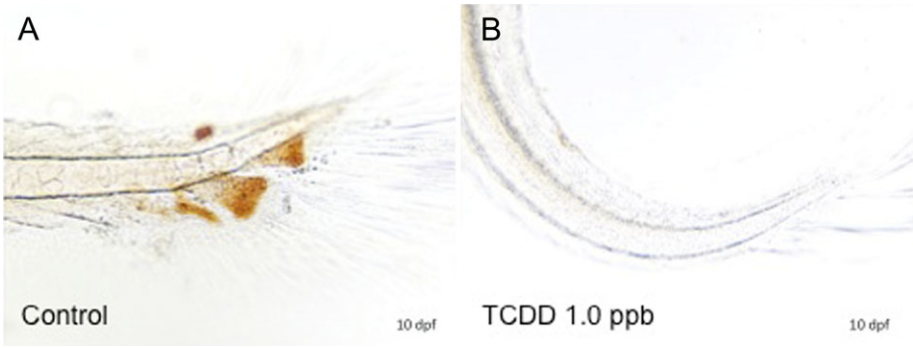

FIG. 4. Effect of TCDD on expression of collagen type II (COL2a) immunoreactivity in medaka hypurals. Embryos were exposed to DMSO (A) or 1 ppb TCDD (B) at 4 hpf for 1 h, washed, and incubated in ERM at 26°C until 10 dpf, at which time, five embryos per group were dechorionated and fixed for WIHC with anti-type II collagen, monoclonal antibody at 1:100. Figures are representative of the five individuals in each group. Brown color indicates positive COL2a immunoreactivity in hypurals. Bar = 100 μm.

partitioning of these genes is unlikely (Fig. 5). Following 1 ppb TCDD treatment, a modest decrease in expression of both *Col2A1* forms was observed within the notochord and caudal end of the tail bud. Reduction in expression, however, was more pronounced for *Col2A1* 1 of 2 than *Col2A1* 2 of 2 indicating that the gene duplicates may possess a differential response to TCDD.

qPCR of Sox9 *and* Col2A1 *Paralogs*

To quantify the impact of TCDD treatment on *Sox9* and *Col2A1* expression, qPCR was conducted on caudal peduncle of individuals at 10 (dpf). Analysis of qPCR results demonstrated that TCDD exposure produced a concentration-dependent decrease in both *Sox9* and *Co2a1* gene paralogs expression when compared with controls of the same age (Figs. 6A–C). Significant concentration-dependent decrease in *Sox9a and Col2a1* 1 of 2 mRNA was observed between 0.05 and 1 ppb TCDD exposure (Figs. 6A and 6B). *Col2a1* 2 of 2 mRNA was less responsive to TCDD with significant decrease in expression occurring at concentrations greater than 0.3 ppb at 10 dpf (6C). No significant difference was observed for *Sox9b* at concentrations examined (data not shown). As a control for exposure, *Cyp1A1* gene expression was assessed in conjunction with *Col2A1*. *Cyp1A1* mRNA expression exhibited a concentration-dependent increase at 10 dpf reaching a maximum of 120× that of controls with 1 ppb TCDD exposures (Supplementary fig. 1).

Proliferating Cell Nuclear Antigen Staining

To assess the impact of TCDD exposures on chondrocyte cell proliferation, immunohistochemistry was conducted using a polyclonal antibody to proliferating cell nuclear antigen (PCNA) on 10 dpf embryonic peduncle sections containing hypural elements. Positive PCNA staining was observed within

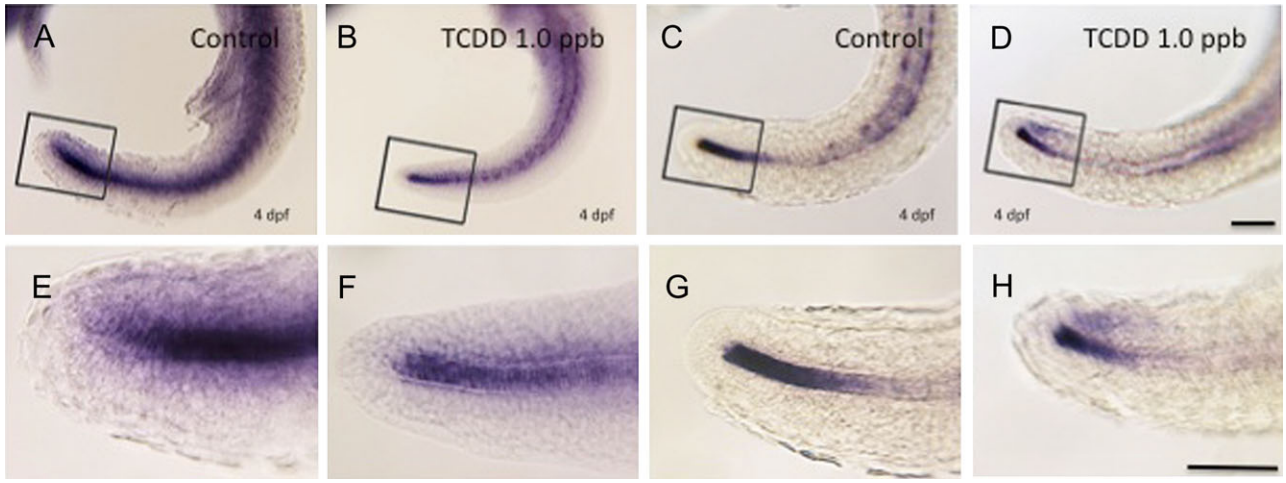

FIG. 5. Expression of *Col2A1* mRNA in caudal peduncle of embryos. Embryos were exposed to DMSO or 1 ppb TCDD at 4 hpf for 1 h, washed, and incubated in ERM at 26°C. At 4 dpf, embryos were dechorionated, fixed, and processed for whole-mount ISH. (A, B, E, and F) *Col2a1* 1 of 2 mRNA expression; (C, D, G, and H) *Col2a1* 2 of 2 mRNA expression. (A, C, E, and G) DMSO controls; (B, D, F, and H) 1 ppb TCDD-exposed embryos. (E–H) are magnifications of the rectangular area indicated in A–D, respectively. Blue coloration indicates *Col2a1* 1 of 2 and *Col2a1* 2 of 2 mRNA expression. Number of animals reacted per group was 10, and representative figures are shown for each group. Bar = 100 μm.

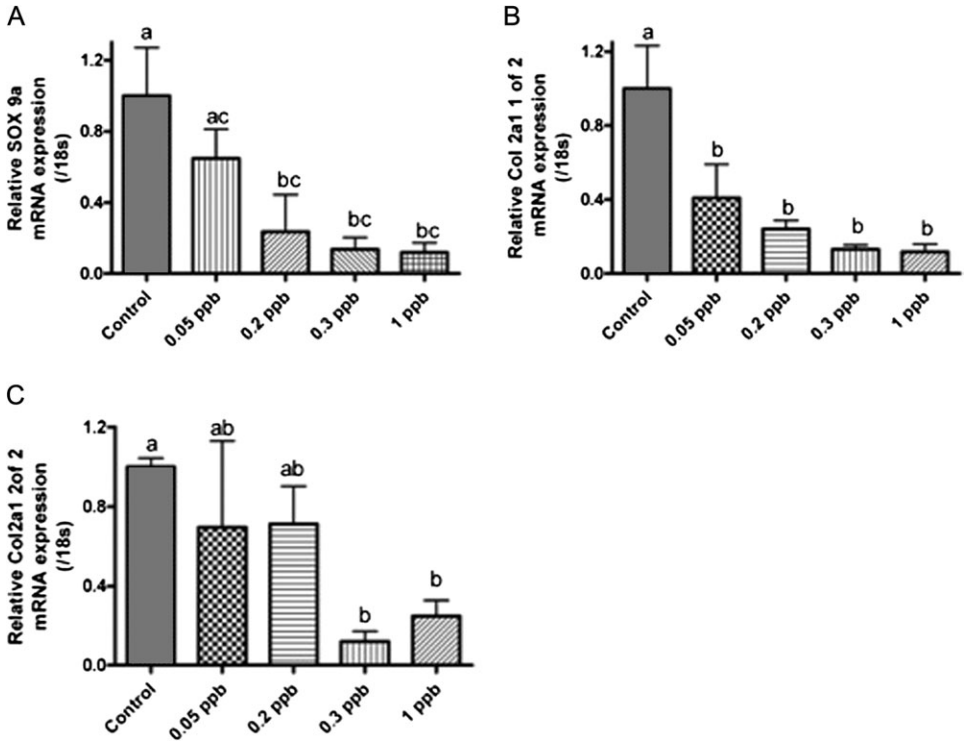

FIG. 6. Quantitative gene expression of *Sox9a* and *Col2A1* in medaka caudal peduncle. Medaka embryos were exposed to DMSO or a graded concentration of TCDD (0.05–1 ppb) at 4 hpf for 1 h, washed, and incubated in ERM at 26°C. At 10 dpf, embryos were dechorionated and caudal peduncles processed for RNA and gene expression as described in ''Materials and Methods.'' (A) Relative *Sox9a* gene expression, (B) relative *Col2A1* 1 of 2 gene expression, and (C) relative *Col2A1* 2 of 2 gene expression. mRNA transcript levels were normalized to medaka 18s and are represented as the mean mRNA level ± SEM. A significant change in transcript was determined using one-way ANOVA, p value < 0.05, followed by Newman-Keuls Multiple Comparison test within the Prism4 software package (GraphPad Software Inc., San Diego, CA). Data were logarithmically transformed as needed to improve equality of variances. All experiments consisted of three replicate experimental wells containing 10 embryo caudal peduncles per well and each experiment was replicated at least three times. All qPCR was conducted in triplicate. Different letters indicate significant differences ($p < 0.05$) between fields.

cartilage anlage within control animals (Fig. 7). PCNA staining localized within the nucleus of a zone of large rounded chondrocytes within the anterior portion of the hypural structure. Staining in this position is consistent with the localization of proliferating/differentiating cells. Chondrocytes within hypural structures of 0.2 ppb TCDD-treated animals failed to stain with the PCNA antibody.

Medaka Skeletogenesis-mCherry Transgenic

To further evaluate skeletal deficits, effects of TCDD exposures on hypural development were determined using the medaka *Osx*-mCherry-transgenic line. mCherry fluorescence in this line is driven through the transcription of the medaka osterix gene promoter (*Osx*). *Osx* is expressed in both mineralized and premineralized osteoblasts as early as stage 28 (2.5 dpf) in developing medaka (Renn and Winkler, 2009). In this study, mCherry fluorescence in hypural structures of control animals (10 dpf) was clearly apparent including HP1, HP2, caudal fin rays in addition to neural, and hemal arches of preural centrum (Fig. 8). This observation is consistent with Renn and Winkler (2009), who observed *Osx*-driven mCherry expression in hypural and fin structures, nonmineralized regions of the fin rays, and distal premineralized borders of the hypurals.

In TCDD-treated medaka, exposure to 0.1 ppb markedly reduced expression of *Osx*-mCherry throughout the tail region and formation of HP2 and both neural and hemal arch structures. *Osx* expression remained in HP1 and caudal fin ray extensions. At a concentration of 0.2 ppb, minimal fluorescence was observed with no discernible hypural or caudal ray fin structures. Neural and hemal arches were absent and caudal peduncular structure appeared homocircular with significant delay in development. TCDD concentrations greater than 0.5 ppb resulted in little to no *Osx*-mCherry expression with extreme deficits in caudal peduncle structure development.

Osx-mCherry positive osteoblasts were also assessed in sections through hypural regions of 10-dpf medaka embryos to detect development of perichondral ossification in these structures. Immunohistochemical detection of *Osx* expressing cells in control animals was observed in periphery of hypural structures, consistent with formation of an ossified sheath surrounding hypural structures through perchondrial ossification (Fig. 9). *Osx* expression was additionally present in the lepidotrichia of fin rays extending from the hypurals.

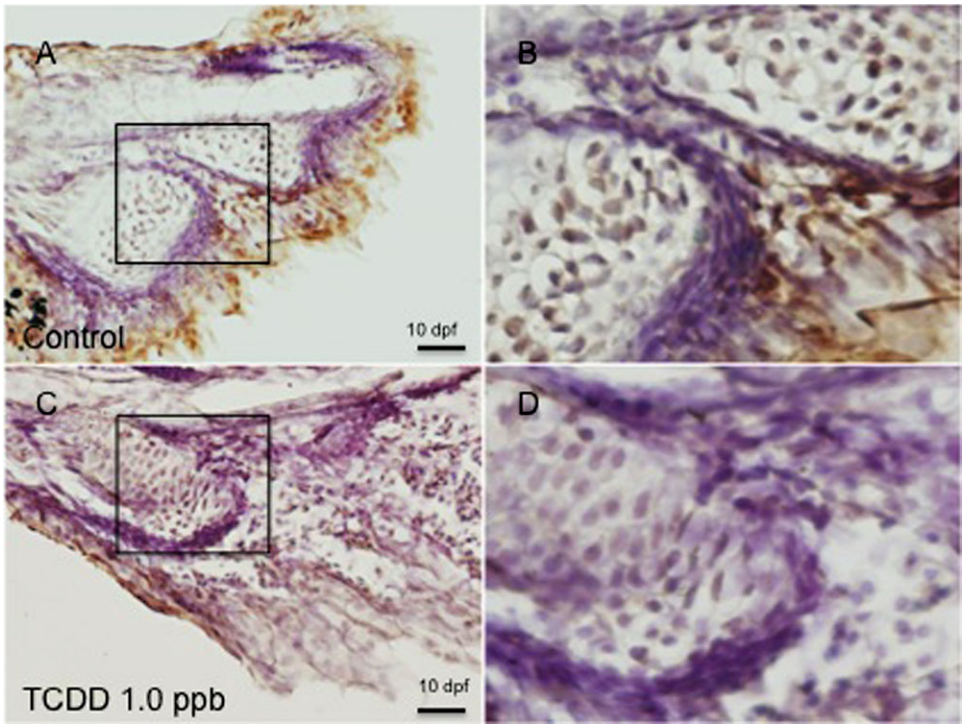

FIG. 7. PCNA immunoreactivity in medaka hypurals. Five individual embryos were exposed to DMSO or 0.2 ppb TCDD at 4 hpf for 1 h, washed, and incubated in ERM at 26°C. At 10 dpf, embryos were dechorionated, fixed, and processed for sectioning and immunohistochemistry as described in ''Materials and Methods.'' (A) DMSO-exposed animals; (C) 1 ppb TCDD-treated animals. B and D are magnifications of the rectangular area indicated in A and C, respectively. Black arrows over nuclei indicates PCNA immunoreactivity in component cells of hypurals. White arrows indicate an absence of PCNA immunoreactivity. Fields shown are representative of all individuals in a given group. Bar = 100 μm.

Conversely, 0.2 ppb TCDD-treated animals exhibited a marked reduction in *Osx* expression within perichondral space of hypural structures indicating a lack of ossification in these structures, however, staining was observed in what appeared to be lepidotrichia within these sections.

DISCUSSION

In this study, we examined the effects of embryonic exposure to TCDD on development of CRHC in hypural structures of medaka caudal peduncles. Previous gross structural assessments of cartilage dysmorphogenesis were investigated in lower and upper jaws (Meckel's, basihyal, paraquadrate) and in cranium of teleosts and shown to be a sensitive endpoint of TCDD toxicity (Carney *et al.*, 2006; Planchart and Mattingly, 2010; Teraoka *et al.*, 2006; Xiong *et al.*, 2008). Less attention, however, has been given to toxicity of TCDD to the axial skeleton. In this investigation, we demonstrate that low concentrations (ppt) of TCDD significantly alter development of cartilage subtypes found in medaka hypural cartilage of the axial tail. Concentrations used in this study are consistent with observed dysmorphogenesis of teleost jaw also containing CRHC and abundant ECM (Planchart and Mattingly, 2010; Teraoka *et al.*, 2006). These data demonstrate that CRHC within jaw and hypural structures is a sensitive target of TCDD toxicity. Our investigation suggests that TCDD significantly reduces cell proliferation and recruitment of mesenchymal cell populations to these structures resulting in dysmorphic and poorly developed hypural cartilage structures. We propose that assessment of hypural cartilage formation is an excellent model to investigate developmental impacts of TCDD on skeletogenesis.

In teleosts, CRHC contains abundant cells with large lacunae surrounded by extensive ECM (Benjamin, 1990, 1989). Morphological analyses of control animals demonstrate that hypural structures have abundant cellular elements (chondrocytes) arranged within the lacunae and surrounded by a defined perichondrium, making them a reasonable model for defined studies of cartilage dysmorphogenesis. We observe that component cells of hypural structures progress through defined stages of cartilage maturation including chondroblast commitment from mesenchymal condensations, cell proliferation, cell differentiation to chondrocytes, and cellular hypertrophy with production of extracellular collagen and aggrecan (Karsenty, 2008). Although some hypertrophic cells appear to be accumulating cell debris, there is no morphologic evidence of apoptosis (viz., bleb formation and/or phagocytosis by adjacent cells). This is consistent with the recent review (Zhang *et al.*,

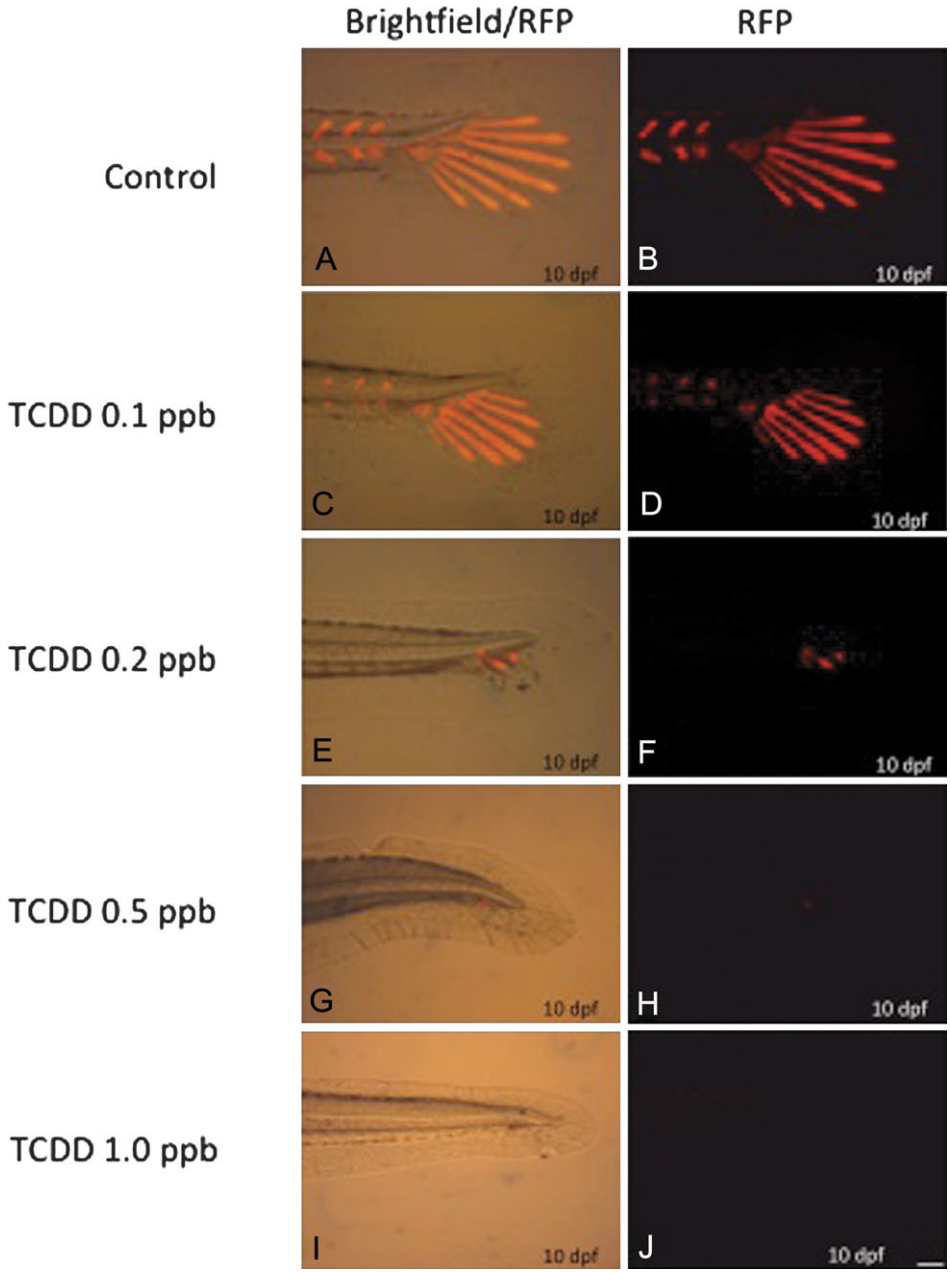

FIG. 8. *Osx*-mCherry transgenic gene expression *in vivo*. *Osx*-mCherry transgenic embryos were exposed to DMSO or a graded concentration of TCDD (0.05–1 ppb) at 4 hpf for 1 h, washed, and incubated in ERM at 26°C. At 10 dpf, embryos were dechorionated, anesthetized in MS222, and imaged *in vivo* using epifluorescent microscopy with a Texas Red filter. B, D, F, H, and J are representative fluorescent images for individuals ($n = 10$ per group). A, C, E, G, and I are overlays of fluorescence and bright field images representative for individuals ($n = 10$ per group). Bar = 100 μm.

2009) of differences between teleosts and mammals. Hypertrophic cells of the latter, but not the former, undergo apoptosis followed by endochondral ossification.

Following TCDD exposure, hypural development was highly attenuated with moderate to little structural maturity. Dysmorphogenesis of hypural cartilage structures proved concentration responsive and highly sensitive, occurring at low ppb levels of TCDD. Our results further demonstrate that TCDD retards and disrupts skeletogenic development at multiple levels, likely involving both chondrogenesis and osteogenesis. Evaluations of hypural chondrocyte formation (GMA histology and TEM) suggest that cellular processes including MSC recruitment/condensation and terminal differentiation of chondrocytes are significantly diminished following TCDD exposure. Additionally, in TCDD-treated animals, hypural cartilage failed to progress toward formation of hypertrophic chondrocytes.

Consistent with these morphological changes, assessment of type II collagen expression in medaka hypurals exhibits

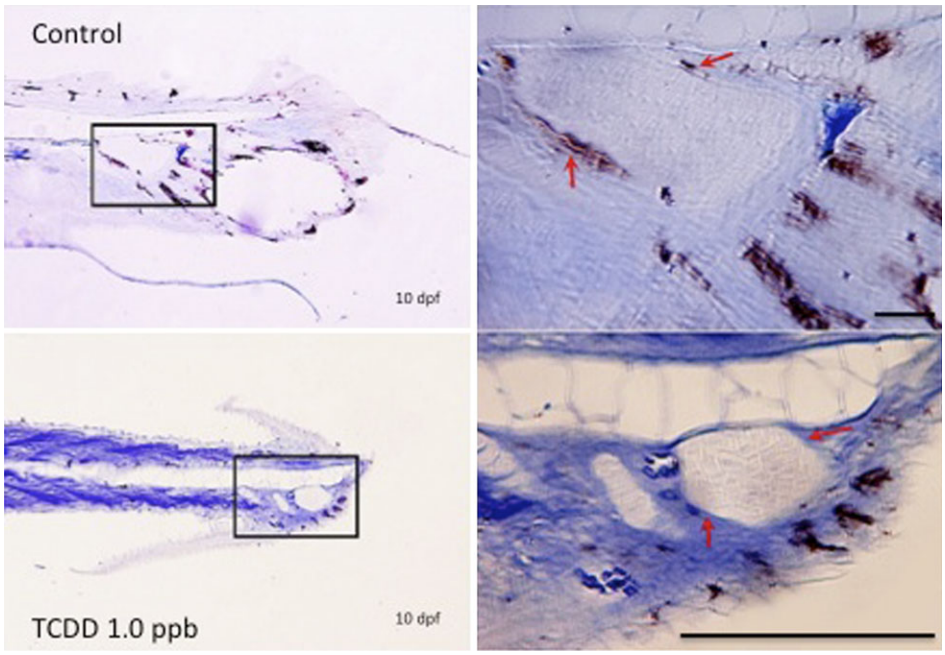

FIG. 9. Assessment of perichondral ossification in medaka hypurals. *Osx*-mCherry transgenic embryos were exposed to DMSO or 1 ppb TCDD at 4 hpf for 1 h, washed, and incubated in ERM at 26°C. At 10 dpf, embryos were dechorionated, fixed, and prepared for immunohistochemical analysis of mCherry gene expression as described in ''Materials and Methods.'' Immunohistochemistry was conducted using a mouse monoclonal anti-RFP antibody. (A and B) DMSO control animals; (C and D) 0.2 ppb TCDD-treated animals. B and D are 40× magnifications of the rectangular area indicated in A and C, respectively. White arrows indicate *Osx* driven mCherry immunoreactivity surrounding hypural structure of controls. Similarly placed white arrows indicate absence of mCherry expression in TCDD-treated animals. $n = 5$ for each group with one representative field chosen for illustration. Bar = 100 μm bar.

a concentration-dependent (qPCR only) decrease. In this study, we used *Col2A* expression as a marker of terminal cartilage development. Regulation of *Col2A* gene expression in teleosts is mediated through SOX9 (Yan *et al.*, 2005). SOX9, a critical chondrogenic transcription factor in fish and mammalian models, plays an integral role in formation of cartilage containing structures by serving as a critical signaling factor in commitment of MSCs toward a chondrogenic lineage (Baek and Kim, 2011). SOX9 directly regulates expression of matrix genes essential to cartilage including type II collagen (COL2A) and aggrecan. Suppression of *Sox9* gene expression in cranial neural crest–derived MSCs blocks cartilage differentiation and enhances ectopic expression of the osteoblast specific markers (Yan *et al.*, 2002, 2005). In this study, we demonstrate significant attenuation in *Sox9a* expression in TCDD-treated hypural structures. These results are consistent with observed downregulation in *Sox9b* expression in zebrafish jaw following TCDD exposures (Xiong *et al.*, 2008). Morpholino knockdown of *sox9b* in zebrafish embryos recapitulated the TCDD-like jaw phenotype and loss of a single copy of the *sox9b* (i.e., *sox9b* (±) heterozygotes) increased sensitivity to jaw malformation by TCDD (Xiong *et al.*, 2008).

We also assessed *Osx* gene expression as a marker of TCDD effects on bone development. Previous studies demonstrated that long-term exposure of juvenile rats to TCDD interferes with bone growth, modeling, and mechanical strength (Jämsä *et al.*, 2001). *In vitro*, bone marrow stem cells treated with TCDD demonstrate reduction in mRNA levels of osteoblast-specific markers suggesting that TCDD disrupts programming associated with differentiation of osteoblasts from MSCs (Korkalainen *et al.*, 2009). Osteoblast differentiation is controlled by a critical set of transcription factors including Runx2 and Osterix (*Osx*) (Akiyama *et al.*, 2002; Komori, 2006). Runx2 is required early in mesenchymal cell commitment toward osteoblasts, whereas *Osx* plays an important regulatory role in terminal osteoblast differentiation (Nakashima *et al.*, 2002). Here, we employed a transgenic medaka model that expresses mCherry under control of the *osterix* promoter. Using this model, *Osx* is expressed normally in medaka premineralized and mineralized bony structures as early as 2.5 dpf (Renn and Winkler, 2009). Following TCDD exposures, we observed a marked attenuation of both *Osx* gene expression and perichondral ossification within the medaka hypurals (10 dpf), and these alterations in caudal peduncle were accompanied by similar changes in other bony structures specifically neural and hemal arches and ossified craniofacial structures (data not shown). These TCDD-induced phenotypes on osteogenesis are consistent with those observed in *Osx* null mice and include a lack of mineralized bone and inability of condensed mesenchyme to fully differentiate into terminally differentiated osteoblasts (Nakashima *et al.*, 2002).

The fact that TCDD impacts both osteogenesis and chondrogenesis suggests that early osteochondroprogenitors may be impacted. However, our observation of expression of

Col2A1 paralogs in 4 dpf–treated animal illustrates that TCDD does not impact initial stages of collagen deposition or formation of cartilage anlage in this model. This effect was also observed in jaw structures of zebrafish where early embryonic exposure to TCDD does not inhibit initial formation of cartilage structures; rather, it impedes subsequent cartilaginous development (Teraoka *et al*., 2002). Interestingly, a similar effect is observed in murine models of TCDD-induced cleft palate where palatal shelves are formed but fail to fuse (Abbott and Birnbaum, 1989). Palatal agenesis is attributed to a decrease in medial epithelial cell proliferation and cell number within embryonic palatal mesenchyme (Abbott and Birnbaum, 1990, 1991; Dhulipala *et al*., 2006; Pratt *et al*., 1984). In this study, our finding of abundant cells positive for PCNA in control hypural chondrocytes indicated significant proliferative activity in these cells. However, consistent with antiproliferative activity of TCDD, treatment of medaka embryos 0.2 ppb TCDD significantly reduced the number of cells positive for PCNA staining in dysmorphic hypural structures at 10 dpf.

Our observation that TCDD exposures result in attenuation in recruitment of mesenchymal cell condensations to the hypural cartilage anlage also suggests that early osteochondroprogenitors may be impacted by exposures. Teleost craniofacial structures, including Meckel's, palatoquadrate, ceratohyal, and hyosymplectic cartilage, are known to be derived from condensations of prechondrogenic neural crest–derived cells within the first and second pharyngeal arches (Yan *et al*., 2002, 2005). Interestingly, these structures, in particular, CRHC observed in the Meckel's structures, proved highly sensitive to TCDD. In contrast, the origin of cells that contribute to formation of axial cartilage are more ambiguous but may include mesenchymal cells of somitic origin, neural or hemal arches, or perhaps trunk somatic mesoderm (Hall and Witten, 2007). The molecular basis of MSC attenuation in TCDD-treated hypurals is unknown. However, several pathways/transcription factors including SOX9 play a critical role(s) in determining the fate of MSCs to osteogenic and chondrogenic cell lineages (Augello and De Bari, 2010). In mice, inactivation of *Sox9* before formation of chondrogenic mesenchymal condensations results in complete absence of mesenchymal condensations and subsequent cartilage and bone formation (Akiyama *et al*., 2002). Conversely, inactivation of *Sox9* after mesenchymal condensations has formed results in a severe chondrodysplasia and an absence of cartilage in the endochondral skeleton (Akiyama *et al*., 2002). Interestingly, those mesenchymal cells expressing *Sox9* prior to MSC condensations are thought to be osteochondroprogenitors.

Teleost models, including medaka and zebrafish, possess duplicate (parologus) copies of *Sox9* (*Sox9a*/*b*) due to successive whole-genome duplication events over the course of vertebrate evolution (Force *et al*., 1999). In the medaka model, we demonstrate that TCDD preferentially attenuates *Sox9a* expression in hypural structures, whereas in zebrafish, TCDD differentially attenuates *Sox9b* expression in jaw homogenates (Xiong *et al*., 2008). Differential expression between *Sox9* duplicates within and between species is likely due to subfunction partitioning of regulatory components within the promoter regions of individual *Sox9* alleles (Cresko *et al*., 2003). Attenuation of medaka *Sox9a* following TCDD exposure suggests that this gene paralog likely contributes to both osteogenic and chondrogenic phenotypes as observed in our skeletogenic model. Duplicate *Sox9* genes may, however, impart a functional redundancy in osteogenic and chondrogenic programs. Conversely, *Sox9* function may have partitioned, in which case each paralog may have a defined yet separate function within the osteogenic and/or chondrogenic program. Attenuation in MSC recruitment to hypural structures in our model may be in part due to downregulation of *Sox9a* gene expression consistent with results obtained with *Sox9* knockout mice. The lack of change in *Sox9b* gene expression following TCDD exposure (this report) indicates this gene paralog may impart a different function within the osteogenic-chondrogenic program. We thus propose that genetic programming involving mesenchymal cell condensation, commitment of MSCs toward osteogenic-chondrogenic lineages and/or terminal differentiation of these cell types in medaka hypurals may be impacted by misregulation of *Sox9a*. In support of this hypothesis, previous studies demonstrate that TCDD blocks regenerative growth of zebrafish caudal fin following partial amputation (Mathew *et al*., 2006). Regenerative failure is accompanied by a reduction in mesenchymal cell recruitment and dysregulation of genes potentially regulated by *Sox9b* (Andreasen *et al*., 2007, 2006).

Much of our understanding of the interplay between genes, their products, and regulatory networks, including those that drive cell fate decisions, such as commitment of MSCs and differentiation of chondroblasts and osteoblasts, are made possible through molecular elucidation of human skeletal dysplasias and mouse knockout models (Karsenty, 2008). However, given that there appears to be significant conservation within skeletogenic networks over the course of evolution, defined role(s) of target genes important in skeletogenesis can now be determined through knockdown and morphometric approaches in additional animal models including teleosts. Although these findings serve to help establish a clear anatomical, cellular, and molecular basis of bone and cartilage development, large data gaps remain in our understanding of the adaptations and modulation of skeletogenesis following toxic insult. Work herein provides a thorough assessment of skeletogenesis in medaka hypural structures following TCDD exposure. We illustrate that CRHC found in hypural structures is a sensitive target of TCDD toxicity. TCDD causes a marked reduction in hypural cartilage development likely due to impairment of cell differentiation and proliferation processes involved in skeletogenic program(s) and responsible for differentiation of MSCs to mature cartilage and bone cells. Many questions remain unresolved regarding the ability of TCDD to disrupt skeletogenesis during development in

mammalian and nonmammalian models. Mechanistic targets of TCDD within these genetic programs and gene X environment interactions will need to be determined in order to relate environmental exposures of TCDD and TCDD-like compounds with skeletal disease etiology. Studies are currently underway to define key transcriptional regulators of chondrogenesis and osteogenesis impacted by TCDD and other TCDD-like compounds using this medaka hypural model.

SUPPLEMENTARY DATA

Supplementary data are available online at http://toxsci.oxfordjournals.org/.

FUNDING

College of Agriculture and Life Sciences at North Carolina State University; National Science Foundation of China; Program for New Century Excellent Talent in University (NSFC: 30360090 and NCET-04-0262 to W.D.).

ACKNOWLEDGMENTS

The *Osx*-mCherry transgenic medaka line was obtained from Christoph Winkler, Department of Biological Sciences, National University of Singapore. We wish to thank Jeanette Shipley-Phillips for her assistance with T.E.M. and Erin Kollitz, Erin Yost, Arnaud Van Wettere, and Gwijun Kwon for medaka care, culture, and maintenance.

REFERENCES

Abbott, B. D., and Birnbaum, L. S. (1989). TCDD alters medial epithelial cell differentiation during palatogenesis. *Toxicol. Appl. Pharmacol.* **99,** 276–286.

Abbott, B. D., and Birnbaum, L. S. (1990). Effects of TCDD on embryonic ureteric epithelial EGF receptor expression and cell proliferation. *Teratology* **41,** 71–84.

Abbott, B. D., and Birnbaum, L. S. (1991). TCDD exposure of human embryonic palatal shelves in organ culture alters the differentiation of medial epithelial cells. *Teratology* **43,** 119–132.

Abel, J., and Haarmann-Stemmann, T. (2010). An introduction to the molecular basics of aryl hydrocarbon receptor biology. *Biol. Chem.* **391,** 1235–1248.

Akiyama, H., Chaboissier, M. C., Martin, J. F., Schedl, A., and de Crombrugghe, B. (2002). The transcription factor Sox9 has essential roles in successive steps of the chondrocyte differentiation pathway and is required for expression of Sox5 and Sox6. *Genes Dev.* **16,** 2813–2828.

Andreasen, E. A., Mathew, L. K., Löhr, C. V., Hasson, R., and Tanguay, R. L. (2007). Aryl hydrocarbon receptor activation impairs extracellular matrix remodeling during zebrafish fin regeneration. *Toxicol. Sci.* **95,** 215–226.

Andreasen, E. A., Mathew, L. K., and Tanguay, R. L. (2006). Regenerative growth is impacted by TCDD: Gene expression analysis reveals extracellular matrix modulation. *Toxicol. Sci.* **92,** 254–269.

Augello, A., and De Bari, C. (2010). The regulation of differentiation in mesenchymal stem cells. *Hum. Gene Ther.* **21,** 1226–1238.

Baek, W. Y., and Kim, J. E. (2011). Transcriptional regulation of bone formation. *Front. Biosci. (Schol. Ed.)* **3,** 126–135.

Benjamin, M. (1989). Hyaline-cell cartilage (chondroid) in the heads of teleosts. *Anat. Embryol. (Berl.)* **179,** 285–303.

Benjamin, M. (1990). The cranial cartilages of teleosts and their classification. *J. Anat.* **169,** 153–172.

Carney, S. A., Prasch, A. L., Heideman, W., and Peterson, R. E. (2006). Understanding dioxin developmental toxicity using the zebrafish model. *Birth Defects Res. Part A Clin. Mol. Teratol.* **76,** 7–18.

Chopra, M., and Schrenk, D. (2011). Dioxin toxicity, aryl hydrocarbon receptor signaling, and apoptosis-persistent pollutants affect programmed cell death. *Crit. Rev. Toxicol.* **41,** 292–320.

Cresko, W. A., Yan, Y. L., Baltrus, D. A., Amores, A., Singer, A., Rodríguez-Marí, A., and Postlethwait, J. H. (2003). Genome duplication, subfunction partitioning, and lineage divergence: Sox9 in stickleback and zebrafish. *Dev. Dyn.* **228,** 480–489.

Dhulipala, V. C., Welshons, W. V., and Reddy, C. S. (2006). Cell cycle proteins in normal and chemically induced abnormal secondary palate development: A review. *Hum. Exp. Toxicol.* **25,** 675–682.

Dong, W., Matsumura, F., and Kullman, S. W. (2010). TCDD induced pericardial edema and relative COX-2 expression in medaka (Oryzias latipes) embryos. *Toxicol. Sci.* **118,** 213–223.

Dong, W., Teraoka, H., Tsujimoto, Y., Stegeman, J. J., and Hiraga, T. (2004). Role of aryl hydrocarbon receptor in mesencephalic circulation failure and apoptosis in zebrafish embryos exposed to 2,3,7,8-tetrachlorodibenzo-p-dioxin. *Toxicol. Sci.* **77,** 109–116.

Dong, W., Teraoka, H., Yamazaki, K., Tsukiyama, S., Imani, S., Imagawa, T., Stegeman, J. J., Peterson, R. E., and Hiraga, T. (2002). 2,3,7,8-Tetrachlorodibenzo-p-dioxin toxicity in the zebrafish embryo: Local circulation failure in the dorsal midbrain is associated with increased apoptosis. *Toxicol. Sci.* **69,** 191–201.

Fernandez-Salguero, P. M., Hilbert, D. M., Rudikoff, S., Ward, J. M., and Gonzalez, F. J. (1996). Aryl-hydrocarbon receptor-deficient mice are resistant to 2,3,7,8-tetrachlorodibenzo-p-dioxin-induced toxicity. *Toxicol. Appl. Pharmacol.* **140,** 173–179.

Fernandez-Salguero, P. M., Ward, J. M., Sundberg, J. P., and Gonzalez, F. J. (1997). Lesions of aryl-hydrocarbon receptor-deficient mice. *Vet. Pathol.* **34,** 605–614.

Force, A., Lynch, M., Pickett, F. B., Amores, A., Yan, Y. L., and Postlethwait, J. (1999). Preservation of duplicate genes by complementary, degenerative mutations. *Genetics* **151,** 1531–1545.

Fujita, K. (1992). Caudal skeleton ontogeny in the Adrianichthyid fish, Oryzias latipes. *Jpn. J. Ichthyol.* **39,** 107–109.

Hall, B. K. (2005). *Bones and Cartilage: Developmental Skeletal Biology*. Elsevier/Academic Press, London, United Kingdom.

Hall, B. K., and Witten, P. E. (2007). *Plasticity of and Transitions Between Skeletal Tissues in Vertebrate Evolution and Development*. Indiana University Press, Bloomington, IN.

Henry, T. R., Spitsbergen, J. M., Hornung, M. W., Abnet, C. C., and Peterson, R. E. (1997). Early life stage toxicity of 2,3,7,8-tetrachlorodibenzo-p-dioxin in zebrafish (Danio rerio). *Toxicol. Appl. Pharmacol.* **142,** 56–68.

Hickok, N. J., Haas, A. R., and Tuan, R. S. (1998). Regulation of chondrocyte differentiation and maturation. *Microsc. Res. Tech.* **43,** 174–190.

Hill, A. J., Bello, S. M., Prasch, A. L., Peterson, R. E., and Heideman, W. (2004). Water permeability and TCDD-induced edema in zebrafish early-life stages. *Toxicol. Sci.* **78,** 78–87.

Hornung, M. W., Spitsbergen, J. M., and Peterson, R. E. (1999). 2,3,7,8-Tetrachlorodibenzo-p-dioxin alters cardiovascular and craniofacial

development and function in sac fry of rainbow trout (Oncorhynchus mykiss). *Toxicol. Sci.* **47,** 40–51.

Inohaya, K., and Kudo, A. (2000). Medaka as a model organism of skeletal development. *Tanpakushitsu Kakusan Koso* **45,** 2745–2751.

Iwamatsu, T. (2004). Stages of normal development in the medaka Oryzias latipes. *Mech. Dev.* **121,** 605–618.

Jämsä, T., Viluksela, M., Tuomisto, J. T., Tuomisto, J., and Tuukkanen, J. (2001). Effects of 2,3,7,8-tetrachlorodibenzo-p-dioxin on bone in two rat strains with different aryl hydrocarbon receptor structures. *J. Bone. Miner. Res.* **16,** 1812–1820.

Karsenty, G. (2008). Transcriptional control of skeletogenesis. *Annu. Rev. Genomics Hum. Genet.* **9,** 183–196.

Komori, T. (2006). Regulation of osteoblast differentiation by transcription factors. *J. Cell. Biochem.* **99,** 1233–1239.

Korkalainen, M., Kallio, E., Olkku, A., Nelo, K., Ilvesaro, J., Tuukkanen, J., Mahonen, A., and Viluksela, M. (2009). Dioxins interfere with differentiation of osteoblasts and osteoclasts. *Bone* **44,** 1134–1142.

Langille, R. M., and Hall, B. K. (1988). Role of the neural crest in development of the cartilaginous cranial and visceral skeleton of the medaka, Oryzias latipes (Teleostei). *Anat. Embryol. (Berl.)* **177,** 297–305.

Lele, Z., and Krone, P. H. (1997). Expression of genes encoding the collagen-binding heat shock protein (Hsp47) and type II collagen in developing zebrafish embryos. *Mech. Dev.* **61,** 89–98.

Livak, K. J., and Schmittgen, T. D. (2001). Analysis of relative gene expression data using real-time quantitative PCR and the 2(-Delta Delta C(T)) Method. *Methods* **25,** 402–408.

Mathew, L. K., Andreasen, E. A., and Tanguay, R. L. (2006). Aryl hydrocarbon receptor activation inhibits regenerative growth. *Mol. Pharmacol.* **69,** 257–265.

Matsumura, F. (2009). The significance of the nongenomic pathway in mediating inflammatory signaling of the dioxin-activated Ah receptor to cause toxic effects. *Biochem. Pharmacol.* **77,** 608–626.

Nakashima, K., Zhou, X., Kunkel, G., Zhang, Z., Deng, J. M., Behringer, R. R., and de Crombrugghe, B. (2002). The novel zinc finger-containing transcription factor osterix is required for osteoblast differentiation and bone formation. *Cell* **108,** 17–29.

Ohisa, S., Inohaya, K., Takano, Y., and Kudo, A. (2010). sec24d encoding a component of COPII is essential for vertebra formation, revealed by the analysis of the medaka mutant, vbi. *Dev. Biol.* **342,** 85–95.

Passeri, M. J., Cinaroglu, A., Gao, C., and Sadler, K. C. (2009). Hepatic steatosis in response to acute alcohol exposure in zebrafish requires sterol regulatory element binding protein activation. *Hepatology* **49,** 443–452.

Peters, J. M., Narotsky, M. G., Elizondo, G., Fernandez-Salguero, P. M., Gonzalez, F. J., and Abbott, B. D. (1999). Amelioration of TCDD-induced teratogenesis in aryl hydrocarbon receptor (AhR)-null mice. *Toxicol. Sci.* **47,** 86–92.

Planchart, A., and Mattingly, C. J. (2010). 2,3,7,8-Tetrachlorodibenzo-p-dioxin upregulates FoxQ1b in zebrafish jaw primordium. *Chem. Res. Toxicol.* **23,** 480–487.

Prasch, A. L., Teraoka, H., Carney, S. A., Dong, W., Hiraga, T., Stegeman, J. J., Heideman, W., and Peterson, R. E. (2003). Aryl hydrocarbon receptor 2 mediates 2,3,7,8-tetrachlorodibenzo-p-dioxin developmental toxicity in zebrafish. *Toxicol. Sci.* **76,** 138–150.

Pratt, R. M., Dencker, L., and Diewert, V. M. (1984). 2,3,7,8-Tetrachloro dibenzo-p-dioxin-induced cleft palate in the mouse: Evidence for alterations in palatal shelf fusion. *Teratog. Carcinog. Mutagen.* **4,** 427–436.

Puga, A. (2011). Perspectives on the potential involvement of the AH receptor-dioxin axis in cardiovascular disease. *Toxicol Sci.* **120,** 256–261.

Puga, A., Ma, C., and Marlowe, J. L. (2009). The aryl hydrocarbon receptor cross-talks with multiple signal transduction pathways. *Biochem. Pharmacol.* **77,** 713–722.

Renn, J., and Winkler, C. (2009). Osterix-mCherry transgenic medaka for in vivo imaging of bone formation. *Dev. Dyn.* **238,** 241–248.

Teraoka, H., Dong, W., Ogawa, S., Tsukiyama, S., Okuhara, Y., Niiyama, M., Ueno, N., Peterson, R. E., and Hiraga, T. (2002). 2,3,7,8-Tetrachlorodibenzo-p-dioxin toxicity in the zebrafish embryo: Altered regional blood flow and impaired lower jaw development. *Toxicol. Sci.* **65,** 192–199.

Teraoka, H., Dong, W., Okuhara, Y., Iwasa, H., Shindo, A., Hill, A. J., Kawakami, A., and Hiraga, T. (2006). Impairment of lower jaw growth in developing zebrafish exposed to 2,3,7,8-tetrachlorodibenzo-p-dioxin and reduced hedgehog expression. *Aquat. Toxicol.* **78,** 103–113.

Teraoka, H., Dong, W., Tsujimoto, Y., Iwasa, H., Endoh, D., Ueno, N., Stegeman, J. J., Peterson, R. E., and Hiraga, T. (2003). Induction of cytochrome P450 1A is required for circulation failure and edema by 2,3,7,8-tetrachlorodibenzo-p-dioxin in zebrafish. *Biochem. Biophys. Res. Commun.* **304,** 223–228.

Tilton, F., La Du, J. K., Vue, M., Alzarban, N., and Tanguay, R. L. (2006). Dithiocarbamates have a common toxic effect on zebrafish body axis formation. *Toxicol. Appl. Pharmacol.* **216,** 55–68.

Xiong, K. M., Peterson, R. E., and Heideman, W. (2008). Aryl hydrocarbon receptor-mediated down-regulation of sox9b causes jaw malformation in zebrafish embryos. *Mol. Pharmacol.* **74,** 1544–1553.

Yamauchi, M., Kim, E. Y., Iwata, H., Shima, Y., and Tanabe, S. (2006). Toxic effects of 2,3,7,8-tetrachlorodibenzo-p-dioxin (TCDD) in developing red seabream (Pagrus major) embryo: An association of morphological deformities with AhR1, AhR2 and CYP1A expressions. *Aquat. Toxicol.* **80,** 166–179.

Yan, Y. L., Miller, C. T., Nissen, R. M., Singer, A., Liu, D., Kirn, A., Draper, B., Willoughby, J., Morcos, P. A., Amsterdam, A., *et al.* (2002). A zebrafish sox9 gene required for cartilage morphogenesis. *Development* **129,** 5065–5079.

Yan, Y. L., Willoughby, J., Liu, D., Crump, J. G., Wilson, C., Miller, C. T., Singer, A., Kimmel, C., Westerfield, M., and Postlethwait, J. H. (2005). A pair of Sox: Distinct and overlapping functions of zebrafish sox9 co-orthologs in craniofacial and pectoral fin development. *Development* **132,** 1069–1083.

Zhang, G., Eames, F. B., and Cohn, M. J. (2009). Evolution of vertebrate cartilage development. *Curr. Top. Dev. Biol.* **86,** 15–41.